ELSEVIER

Earth and Planetary Science Letters 203 (2002) 999–1014

EPSL

www.elsevier.com/locate/epsl

Dissolved and particulate ^{231}Pa and ^{230}Th in the Atlantic Ocean: constraints on intermediate/deep water age, boundary scavenging, and ^{231}Pa/^{230}Th fractionation

S.B. Moran [a,*], C.-C. Shen [b], H.N. Edmonds [c], S.E. Weinstein [a], J.N. Smith [d], R.L. Edwards [e]

[a] *Graduate School of Oceanography, University of Rhode Island, Narragansett, RI 02882-1197, USA*
[b] *Department of Geosciences, National Taiwan University, Taipei 106, Taiwan, R.O.C.*
[c] *Marine Science Institute, University of Texas at Austin, Port Aransas, TX 78373-5015, USA*
[d] *Marine and Environmental Sciences Division, Bedford Institute of Oceanography, Dartmouth, NS, Canada B2Y 4A2*
[e] *Department of Geology and Geophysics, University of Minnesota, Minneapolis, MN 55455, USA*

Received 30 January 2002; received in revised form 2 August 2002; accepted 19 August 2002

Abstract

^{231}Pa and ^{230}Th concentrations were determined in filtered seawater and suspended particulate matter collected from the Labrador Sea and the Equatorial and South Atlantic to constrain their application as tracers of intermediate/deep water age and Atlantic thermohaline circulation. Distributions of total ^{231}Pa and ^{230}Th indicate the influence of recently formed North Atlantic Deep Water, as evidenced by nearly invariant concentrations below ~1000 m in the Labrador Sea and increasing ^{231}Pa and ^{230}Th concentrations as deep waters progress southward from northern source regions. Application of a scavenging–mixing model to both tracer distributions indicates an intermediate/deep water age of 12 yr in the Labrador Sea and a ~30–140 yr transit time to the low-latitude stations. We attribute a striking increase in total ^{230}Th in the Labrador Sea from 1993 to 1999 to aging of intermediate waters as a consequence of the cessation of deep convection in the Labrador Sea since 1993. The temporal change in the ^{230}Th age of these waters is consistent with the 6 yr time interval between the observations. The average particulate ^{231}Pa/^{230}Th activity ratio in the Labrador Sea and low-latitude deep waters is 0.057 ± 0.003, significantly below the ^{231}Pa/^{230}Th production ratio (0.093) and in agreement with excess ^{231}Pa/^{230}Th ratios in Holocene sediments (0.060 ± 0.004) and sediment trap material (0.034 ± 0.012) from the Atlantic and model simulations. This observation is consistent with the southward transport of deep water strongly attenuating boundary scavenging in the Atlantic. A latitudinal dependence in particle fractionation of these tracers is also evident, with elevated fractionation factors ($F_{Th/Pa}$) observed near the Equator and South Atlantic gyre (~11) compared to low values in the Labrador Sea (~3) and Southern Ocean (~2). There also exists a depth dependence in $F_{Th/Pa}$, characterized by low values in surface waters, a broad mid-depth maximum, and decreasing values towards the sea-floor. The latitudinal and depth variations in $F_{Th/Pa}$ are suggested to reflect differences in the chemical composition of marine particles.

* Corresponding author. Tel.: +1-401-874-6530; Fax: +1-401-874-6811.
E-mail address: moran@gso.uri.edu (S.B. Moran).

0012-821X/02/$ – see front matter © 2002 Elsevier Science B.V. All rights reserved.
PII: S0012-821X(02)00928-7

Keywords: Atlantic Ocean; radioactive isotopes; ventilation; thermohaline circulation

1. Introduction

An understanding of the intermediate/deep water age and circulation of the Atlantic is central to constraining models of the strength of the global thermohaline circulation and climate change. Several recent investigations have reported that the particle-reactive radionuclides ^{231}Pa (half-life 32.8 kyr) and ^{230}Th (half-life 75.5 kyr), produced uniformly by alpha decay of ^{235}U and ^{234}U, respectively, may be used as tracers of intermediate/deep water age [1–7] and the intensity of Atlantic thermohaline circulation through the last glacial termination [8,9]. In ocean basins such as the northern Atlantic, where water mass residence times are similar to the scavenging residence times of ^{230}Th (~20–40 yr) and ^{231}Pa (~50–200 yr) [10–13], the distributions of these tracers are particularly sensitive to deep water age [1,4,5–7].

The influence of newly formed North Atlantic Deep Water (NADW) on the lateral redistribution of these tracers in the Atlantic has been suggested based on low excess sediment ^{231}Pa/^{230}Th ratios observed in both the interior basins and oceans margins north of 50°S [8,14]. Moreover, low excess ^{231}Pa/^{230}Th ratios in Atlantic sediments from the Holocene and the Last Glacial Maximum (LGM) have been interpreted as implying a similar rate of NADW production during the LGM [8]. This conclusion is in conflict with benthic δ^{13}C and Cd/Ca data that point to a reduced production of NADW during the LGM [15,16], though a recent analysis suggests that uncertainties in sedimentary ^{231}Pa/^{230}Th ratios are too large to rule out a 50% decrease in the strength of the Atlantic thermohaline circulation during the LGM [9].

In addition to their potential as tracers of water mass age in the modern and last glacial Atlantic, high-resolution down-core measurements of excess sediment ^{231}Pa/^{230}Th ratios may be able to resolve abrupt changes (~500–1000 yr) in the strength of NADW production, such as associated with the Younger Dryas and Heinrich events, over the past ~150 kyr [6,8,9]. A critical assumption in the application of excess sediment ^{231}Pa/^{230}Th as a tracer of past changes in Atlantic thermohaline circulation is the existence of a constant chemical fractionation of these tracers between seawater and the solid phases that control their scavenging removal. Evidence from laboratory experiments [17] and field observations [14,18,19], however, indicates that the chemical composition of particles may significantly influence the solid-solution partitioning of these tracers. A key question is the extent to which geographical variations in the chemical composition of particles may affect ^{231}Pa/^{230}Th fractionation and hence their use as a proxy of thermohaline circulation in the modern and past Atlantic.

The application of ^{231}Pa and ^{230}Th as tracers of the intensity of past changes in Atlantic intermediate/deep water formation and circulation requires a detailed understanding of their water column distributions and the processes controlling them. In this work, we compare measurements of dissolved and particulate ^{231}Pa and ^{230}Th undertaken in 1999 in the Labrador Sea with results from proximal locations in this basin undertaken in 1993 [6] and contrast them with measurements in 1996 from the Equatorial and South Atlantic. The water column ^{231}Pa and ^{230}Th data provide a confirmation of sedimentary ^{231}Pa/^{230}Th ratios in the Atlantic [8], an improved estimate of the export of ^{231}Pa and ^{230}Th from the North Atlantic to the Southern Ocean, and further support for their use as tracers of Atlantic thermohaline circulation.

2. Methods

Seawater samples were collected at six stations (IOC-6, 8, 10, RFZ, Amazon 1, 2) in the Equatorial and South Atlantic during May–June 1996, as part of the 1996 Intergovernmental Oceanographic Commission (IOC) Baseline Contaminants program. Samples were also collected

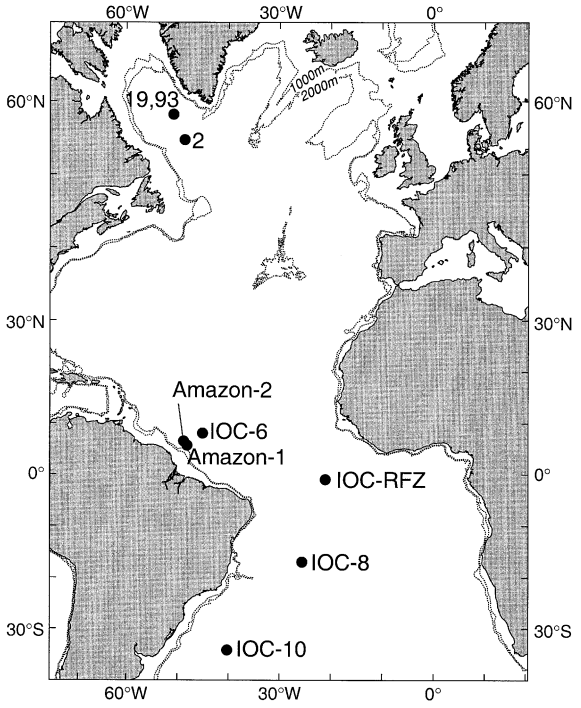

Fig. 1. Map showing sampling stations occupied in the Labrador Sea and Equatorial and South Atlantic. Samples were collected in the Labrador Sea at St. 93 in 1999, and at St. 2 and St. 19 in 1993. Samples were collected from the Equatorial and South Atlantic in 1996.

from the central Labrador Sea (St. 93) in June–July 1999, along the WOCE AR07W transect. This station is located approximately 4° north of St. 2 occupied in 1993 (Fig. 1), where high precision dissolved and particulate ^{230}Th and ^{232}Th data have been reported [6].

Sampling was conducted using clean techniques to minimize sources of contamination. Sample manipulations at sea were conducted in a laminar-flow bench. In the Equatorial and South Atlantic, seawater was collected using Go-Flo bottles modified for trace metal sampling and deployed on a Kevlar hydrowire, whereas a stainless steel hydrowire was used in the Labrador Sea. Seawater was filtered from the Go-Flo bottles using N_2 over-pressure through either acid-cleaned 0.4-μm, 90-mm diameter Teflon filters (Equatorial and South Atlantic), or acid-cleaned 0.4-μm, 47-mm and 142-mm diameter Nuclepore filters (Labrador Sea). Filters were held in teflon filter holders. Filtered seawater samples (1–2 l) were stored acidified. Filters containing particulate matter filtered from 10–20 l of seawater were rinsed with pH 8 Milli-Q water to remove salts and stored frozen in plastic bags until further processing in the shore-based laboratory.

The techniques used for chemical purification of Pa and Th in filtered seawater and particulate samples have been previously described [5–7,20–24]. ^{231}Pa and ^{230}Th abundances were quantified using a Finnigan MAT 262 RPQ thermal ionization mass spectrometer in pulse counting mode. ^{230}Th and ^{232}Th in particulate samples were also measured using a Finnigan MAT ELEMENT sector-inductively plasma mass spectrometer with a CETAC MCN-6000 desolvation nebulizer [23]. Chemical blanks for the dissolved fraction were 0.47 ± 0.10 fg ^{230}Th (2–20% of sample), 0.016 ± 0.016 fg ^{231}Pa (1–20% of sample), and 2.40 ± 0.50 pg ^{232}Th (2–19%) [23,24]. For the particulate fraction, procedural blanks were: 0.45 ± 0.09 fg ^{230}Th, 0.016 ± 0.015 fg ^{231}Pa, and 2.4 ± 0.5 pg ^{232}Th using Teflon filters; 3.0 ± 0.2 fg ^{230}Th, 0.090 ± 0.020 fg ^{231}Pa, and 14.7 ± 0.4 pg ^{232}Th using 47-mm Nuclepore filters, and; 3.0 ± 0.2 fg ^{230}Th, 0.150 ± 0.020 fg ^{231}Pa, and 53 ± 3 pg ^{232}Th using 142-mm Nuclepore filters. Uncertainties in the ^{231}Pa, ^{230}Th and ^{232}Th data were calculated at the 2σ level and include corrections for blanks, multiplier dark noise, abundance sensitivity, and ^{231}Pa, ^{230}Th and ^{232}Th in the respective ^{233}Pa and ^{229}Th spikes.

3. Results

3.1. Labrador Sea

Hydrographic characteristics of the Labrador Sea at St. 93 are illustrated in depth profiles of salinity and dissolved silicate (Fig. 2). The surface layer is characterized by minimum values in salinity and silicate, which increase sharply with depth to form subsurface maxima at ~250 m. The increase in salinity and silicate between ~500–1900 m represents Labrador Sea Water (LSW). Below the LSW is the more saline, nutrient rich, North-

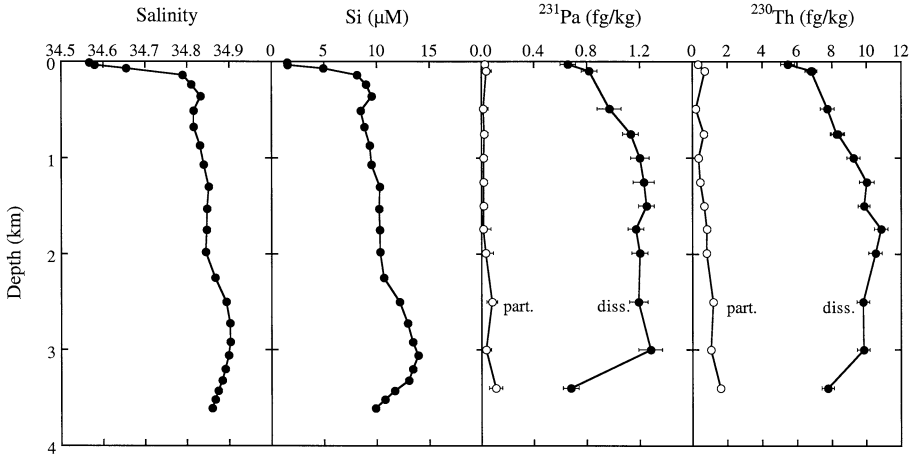

Fig. 2. Depth profiles of salinity, dissolved silicate, and dissolved and particulate ^{231}Pa and ^{230}Th concentration in the Labrador Sea.

east Atlantic Deep Water (NEADW), which extends from ~2200–3300 m and shows a slight salinity and silicate maximum between ~2900–3100 m. The nutrient-depleted, low-salinity Denmark Strait Overflow Water (DSOW) is evident within the bottom ~100 m.

Dissolved ^{231}Pa and ^{230}Th concentrations in the Labrador Sea range from 0.66–1.28 fg/kg and 5.48–10.85 fg/kg, respectively (data may be obtained from the **Background Data Set**[1]). Particulate ^{231}Pa and ^{230}Th represent 1–5% and 3–12% of the respective dissolved concentrations, with the exception of the bottom water sample where particulate ^{231}Pa and ^{230}Th increases to 16% and 21%, respectively, of the dissolved fraction. Vertical profiles of dissolved ^{231}Pa and ^{230}Th concentration are characterized by low values in the surface waters and a progressive increase with depth down to ~1000 m (Fig. 2). Below this depth, dissolved ^{231}Pa and ^{230}Th concentrations are essentially invariant, except in the DSOW, which has lower dissolved values. Particulate ^{230}Th and ^{231}Pa concentrations exhibit a slight increase with depth throughout the water column.

3.2. Equatorial and South Atlantic

Salinity and dissolved silicate profiles for the IOC-96 stations are plotted in Fig. 3. Stations IOC-8 and IOC-RFZ (IOC station located at the Romanche Fracture Zone) have salinity and silicate distributions that essentially lie within those described for IOC-6 and IOC-10 [25]. The upper waters (< 500 m) are characterized by salinity maxima and silicate minima. Salinity decreases and silicate increases below this depth into the core of the Antarctic intermediate water between ~750–900 m. Circumpolar Deep Water (CPDW) lies below these depths, as indicated by the elevated silicate concentrations at 1500 m at IOC-10 and ~1000 m at IOC-6, 8 and RFZ. Silicate concentrations are lower below CPDW, due to the presence of NADW between 2200–3200 m at IOC-10, 1600–4200 m at IOC-6, 1600–3500 m at IOC-8, and 1600–4000 m at IOC-RFZ. In the deeper waters, high-silicate, low-salinity Antarctic bottom water is clearly evident.

Dissolved ^{231}Pa and ^{230}Th concentrations range from 0.33–3.95 fg/kg and 2.32–29.45 fg/kg, respectively. Particulate ^{231}Pa and ^{230}Th represent ~1–3% and ~6–24% of the dissolved concentration, except in the bottom waters at IOC-10 (4350 m and 4500 m) where particulate ^{231}Pa and ^{230}Th increase to 9% and 40%, respectively, of the dissolved fraction, possibly due to sediment resuspension. Vertical profiles of dissolved ^{231}Pa exhibit increasing concentrations from the surface waters down to ~1000–2000

[1] http://www.elsevier.com/locate/epsl

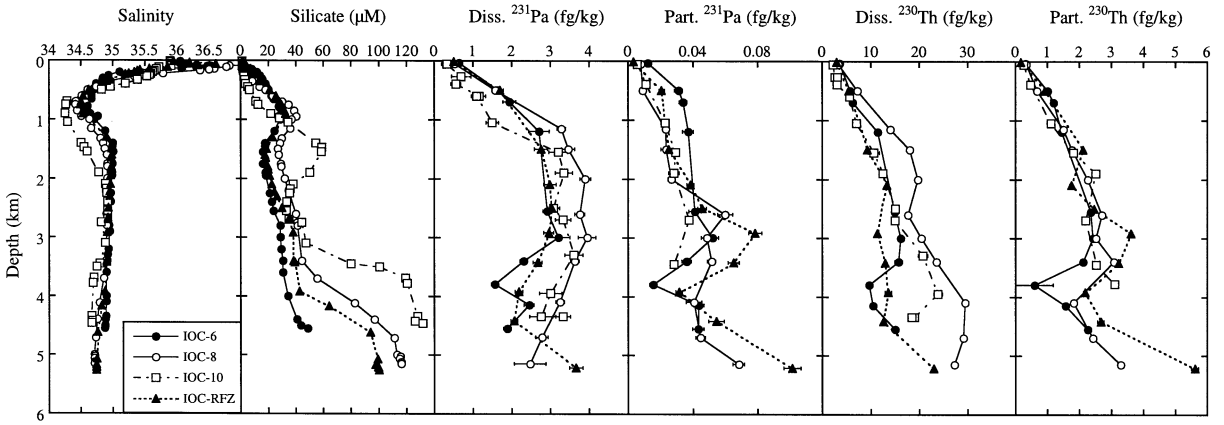

Fig. 3. Depth profiles of salinity, dissolved silicate, and dissolved and particulate ^{231}Pa and ^{230}Th concentration in the Equatorial and South Atlantic.

m (Fig. 3). Below this depth, dissolved ^{231}Pa is nearly constant down to ~3000 m and then decreases toward the ocean bottom. Dissolved ^{230}Th profiles are characterized by minimum values in the surface waters and a progressive increase with depth to ~2000 m. Below these depths, dissolved ^{230}Th concentrations exhibit more variability between stations. Dissolved ^{230}Th concentrations are invariant down to 4500 m at IOC-RFZ, whereas values tend to increase down to 4000 m at IOC-10. At IOC-6, dissolved ^{230}Th exhibits a concave distribution within the bottom 1500 m, whereas the reverse is observed at IOC-8. Distributions of particulate ^{231}Pa and ^{230}Th essentially follow the distribution of the respective dissolved fractions, though a broad minimum is observed between ~3500–4500 m. Note that the high particulate ^{231}Pa and ^{230}Th concentrations at 4350 m and 4500 m at IOC-10 are off-scale and not plotted in Fig. 3.

Concentrations of ^{230}Th are within the range of measurements reported for the Norwegian Sea [5], Labrador Sea [6], western North Atlantic [26], and Southern Ocean [1], and with results from GCM modeling of ^{230}Th distributions in the Holocene Atlantic [27]. Concentrations of ^{231}Pa are slightly lower than or similar to values reported for the Southern Ocean [1] and consistent with recent results from the central Atlantic [28].

3.3. Amazon plume particulate ^{231}Pa and ^{230}Th

Particulate ^{231}Pa and ^{230}Th concentrations determined in the upper few hundred meters at station Amazon-1 and 2 are similar to those determined at similar depths at stations further offshore. No filtered seawater samples were collected at these stations. The upper waters at these stations were reported to have characteristics (low salinity, elevated silicate) indicative of a plume originating from the Amazon River [25].

3.4. Dissolved and particulate ^{232}Th

Dissolved and particulate ^{232}Th concentrations in the Labrador Sea and Equatorial and South Atlantic range from 12.89–132.56 pg/kg and 5.30–148.6 pg/kg, respectively. Vertical profiles of dissolved ^{232}Th are similar at all stations occupied, characterized by variable concentrations in the surface waters, a slight mid-depth minimum, and increasing values toward the ocean bottom (Fig. 4). Depth profiles of particulate ^{232}Th are also similar for all stations occupied, though they reveal less vertical structure. Particulate ^{232}Th concentrations are generally higher at the Amazon stations compared to similar depths further offshore. The close range in concentration and vertical structure observed for all ^{232}Th profiles suggest that external contamination was insignificant. This is important as ^{232}Th is consider-

ably more difficult to control for contamination than ^{231}Pa and ^{230}Th, due to its external source and higher crustal abundance. This also suggests that contamination during sampling and shipboard processing was not significant for ^{231}Pa and ^{230}Th for the Labrador Sea and IOC-96 expeditions, and that these data are directly comparable from the standpoint of contamination.

4. Discussion

4.1. Influence of intermediate/deep water age on water column ^{231}Pa and ^{230}Th distributions

The factors affecting the oceanographic distributions of ^{231}Pa and ^{230}Th are in situ production, scavenging removal by sinking particles, particle composition, advection, diffusion and water mass age. Scavenging residence times of ^{230}Th and ^{231}Pa in deep waters are ~20–40 yr and ~50–200 yr, respectively, which reflects the lower particle reactivity of Pa ($K_d \sim 10^5$) compared to Th ($K_d \sim 10^6$–10^7) [10–13]. The differential scavenging residence times of these tracers give rise to marked variations in their water column distributions and accumulation in the sediments, which can vary significantly as a function of particle flux, particle composition and water mass age.

Thus, in ocean basins where intermediate and deep water ages are in excess of several hundred years, such as the Pacific, profiles of ^{230}Th increase with depth throughout the water column, due to production from ^{234}U and reversible exchange of ^{230}Th between solution and sinking particles [10,29]. The concentration of total ^{230}Th can be modeled according to [10]:

$$C_t = \frac{P}{SK} z \quad (1)$$

where C_t is the total ^{230}Th concentration, P is the ^{230}Th production rate ($P_{Th} = 0.56$ fg/kg/yr $= 2.8 \times 10^{-5}$ dpm/kg/yr), S is the particle-settling rate (m/yr), K is the ratio of particulate to total concentration, and z is the water depth

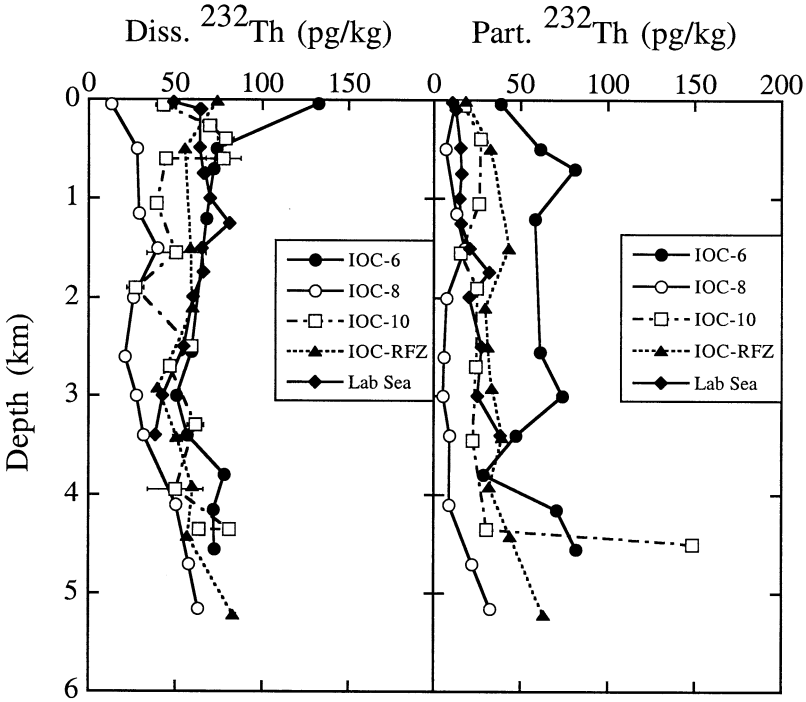

Fig. 4. Depth profiles of dissolved and particulate ^{232}Th concentration in the Labrador Sea and Equatorial and South Atlantic.

[10,29]. Lateral transport of ^{230}Th via advection and diffusion is assumed to be negligible in this case, and the flux of ^{230}Th to the sediments is equal to its production rate in the overlying water column [30]. This assumption has been made when estimating the collection efficiency of deep ocean sediment traps [30–32].

Unlike ^{230}Th, distributions of ^{231}Pa exhibit a greater degree of variability in older intermediate/deep waters and marked differences from the reversible-exchange scavenging model [13]. In the Pacific, ^{231}Pa concentrations increase down to ~1500–2000 m and are invariant below this depth [13], whereas concentrations increase throughout the water column in the Arctic Ocean [2,3]. Departures from linearity reflect the longer scavenging residence time for ^{231}Pa compared to ^{230}Th, allowing lateral transport from oligotrophic central gyres to higher productivity regions (upwelling areas, ocean margins) where ^{231}Pa is more effectively scavenged from the water column.

In ocean basins where the water mass residence time is similar to the scavenging residence times of ^{231}Pa and ^{230}Th, their distributions reflect departures from scavenging models that predict a linear increase with depth. In particular, the influence of low water mass ages on the water column distributions of ^{231}Pa and ^{230}Th in intermediate and deep waters has been observed in Atlantic, Arctic and Antarctic ocean basins [1–7,26,33]. In the present study, a scavenging–mixing model can be used to calculate water mass ages of recently formed Labrador Sea intermediate/deep waters and their transit time to the Equatorial and South Atlantic regions [6,7]. The material balance for total ^{230}Th or ^{231}Pa (C_t) at steady-state is [1,6,7],

$$C_t = (P\tau_w + C_i)(1-e^{-z/\tau_w SK}) \quad (2)$$

where C_i is the initial ^{230}Th or ^{231}Pa concentration in northern source waters, τ_w is the water mass age, $P_{Pa} = 0.0217$ fg/kg/yr (2.33×10^{-6} dpm/kg/yr), and the other variables are as described above. The initial ^{230}Th concentration was set at 4.5 fg/kg, based on previous measurements from the Denmark Strait overflow waters [5]. Direct measurements of ^{231}Pa have not been reported for the Denmark Strait and Iceland–Scotland overflow waters, and C_i^{Pa} was set at 1 fg/kg, based on the concentration in the Labrador Sea (Fig. 2) at depths similar to the overflow sill depth of 500 m. The ^{231}Pa concentration in newly formed overflow waters is likely to be a reasonable estimate, though this remains to be confirmed. Model profiles of total ^{231}Pa and ^{230}Th were calculated for each station using the average measured K_{Pa} and K_{Th} values and an estimated particle settling rate of $S = 500$ m/yr, which is within the range of reported values [1,4,6,10,13,29].

This simple model (Eq. 2) describes a one-dimensional system, an ocean water column, and considers reversible scavenging of ^{231}Pa and ^{230}Th and water mass age. In applying the model to the Atlantic, the assumption is that the system starts at time $t = 0$ in the northern source waters and moves southward with time. Note that the term 'mixing' in the scavenging–mixing model is intended to represent the net effect of the aging of the water mass, which occurs via advection and diffusion during southward transit. The model describes the steady-state situation at a point along a pipe-flow reactor, where transport of material normal to the flow is permitted and represents the effect of scavenging removal of ^{231}Pa and ^{230}Th by sinking particles. The vertical profiles of ^{231}Pa and ^{230}Th along the flow path reflect the net imbalance between production by U decay and removal by scavenging in the presence of a steady unidirectional transport. Lateral exchange with water outside of the one-dimensional system is not permitted. Eq. 2 is intended to be used to evaluate the large-scale effects of reversible scavenging and water mass age on intermediate/deep water distributions of total ^{231}Pa and ^{230}Th. This model, with lateral flushing of Atlantic deep water from a northern source, would not reproduce fine-scale features above the main thermocline [6]. Rather, the primary purpose of this model is to illustrate the effect of particle scavenging and water mass age on ^{231}Pa and ^{230}Th distributions in the intermediate/deep Atlantic.

In the Atlantic, water mass ages calculated using ^{231}Pa and ^{230}Th distributions provide a measure of the average transit time of ^{231}Pa and ^{230}Th-depleted surface waters injected from the

overflow regions into the deep waters. In this case, the ^{231}Pa–^{230}Th water mass age can approximate a ventilation age as determined using tracers such as CFC's and He/^{3}H ratios, which are established solely by the time elapsed since contact with the atmosphere. Furthermore, while tracer ages determined using CFC's, He/^{3}H ratios and ^{231}Pa/^{230}Th are intended to provide a measure of the timescale of water mass movement, all are complicated by mixing. Finally, it is important to recognize that, because ^{231}Pa and ^{230}Th are particle-reactive and hence non-conservative in the oceans, these water mass tracer ages may deviate from air–sea interaction tracers of ventilation as a result of any large-scale scavenging removal that may occur (e.g., near upwelling areas and ocean boundaries) during southward transport.

4.2. Constraints on water mass age in the Atlantic

Before comparing the model results with the ^{230}Th observations in the Labrador Sea, it is important to consider the hydrographic properties at the station locations occupied in 1993 and 1999 (Fig. 5). In 1993, ^{230}Th samples were collected at St. 2 [6], which is approximately 4° south of St. 93 in 1999. Profiles of salinity and silicate at St. 2 and St. 93 as well as St. 19 in 1993, the same location as St. 93, are virtually identical; the only slight difference is silicate in NEADW. Thus, the water masses sampled in 1993 and 1999 are regarded as the same with respect to their hydrographic properties.

This is not the case for CFC-11 concentrations, which are low (and similar) at St. 2 and St. 19 in 1993 compared to higher values in both LSW and NEADW at St. 93 in 1999 (Fig. 5). The atmospheric input function for CFC-11 increased almost linearly with time between 1970 and 1990 and has remained relatively constant since the early 1990's. Active convection in the Labrador Sea in 1993–94 resulted in ventilation of the water column to a depth of 2200 m. This eliminated the vertically decreasing CFC-11 concentration gradient that had been previously established in the upper 2000 m during previous years of reduced convection. Between 1993–94 and 1999, convection was limited to the upper 1500 m (referred to as 'new' LSW) and CFC-11 levels in this water mass gradually increased as they equilibrated with atmospheric levels [34]. CFC-11 levels in 'old' LSW (1500–2300 m) remained relatively constant at levels consistent with the 1993–94 period of intense convection. Azetsu-Scott et al. [34] have estimated ventilation ages, based on CFC-12 distributions (80% saturation) for 'new' and 'old'

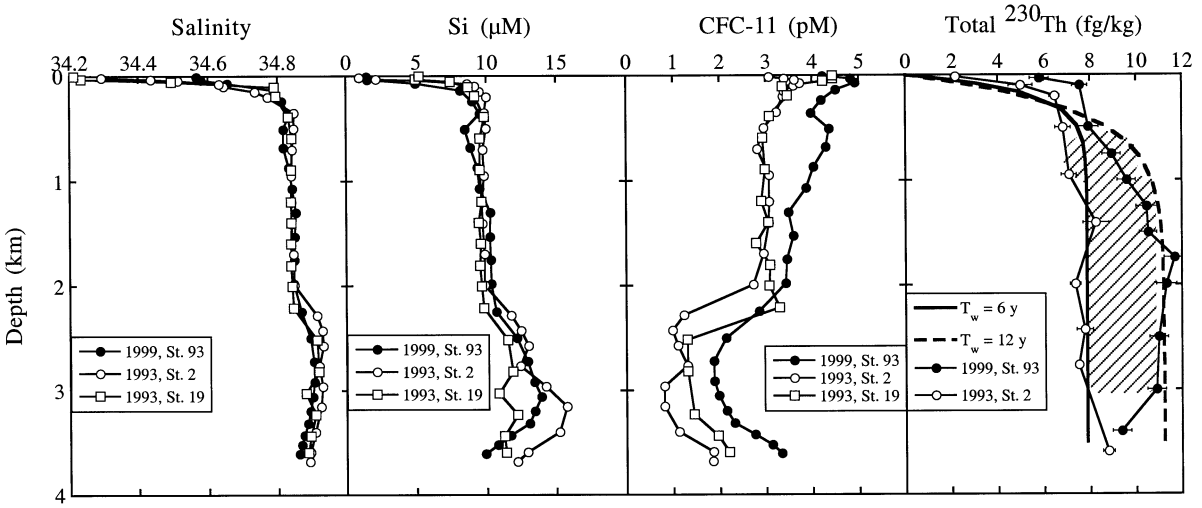

Fig. 5. Depth profiles collected in 1993 and 1999 in the Labrador Sea of salinity, silicate, CFC-11 and total ^{230}Th concentration compared with the scavenging–mixing model (Eq. 2).

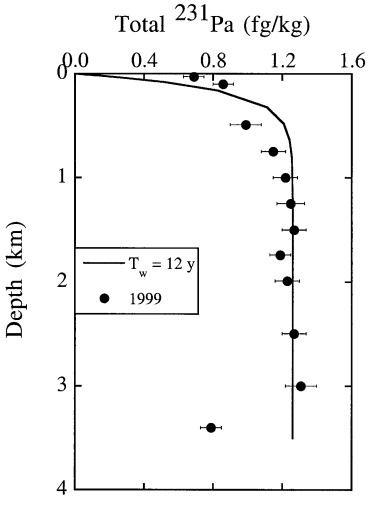

Fig. 6. Depth profile of total ^{231}Pa collected in 1999 in the Labrador Sea compared with the scavenging–mixing model (Eq. 2).

LSW, to be 2 yr and 8 yr, respectively. Azetsu-Scott et al. [34] have also estimated mean CFC-12 ventilation ages (80% saturation) of 21 yr and 15 yr for NEADW and DSOW, respectively, in the Labrador Sea. The 1993–99 increase in the CFC-11 concentrations in both water masses can be attributed to the increase in the CFC-11 atmospheric input function during the 1970's [35]. Thus, the CFC data are interpreted as indicating that deep water in 1999 was six years older than in 1993, implying a full stop of deep convection in 1993.

Distributions of ^{230}Th also exhibit a striking increase throughout the water column between 1993 and 1999 (Fig. 5). ^{230}Th distributions for 1993 and 1999 have been simulated using the average measured values $K_{Th} = 0.067$ [5] and $K_{Th} = 0.055$ and deep water ages of $\tau_w = 6$ years and $\tau_w = 12$ yr, respectively. The good agreement between the model and experimental results suggests that the absence of deep convection in LSW between 1993 and 1999 is equivalent from a modeling perspective to an increase in the water mass age from 6 yr to 12 yr. There is no evidence indicating that ventilation ages in NEADW changed significantly between 1993 and 1999, yet the ^{230}Th concentration between 2400 m and 3000 m increased markedly during this period. Despite having a relatively old ventilation age, however, NEADW has probably been in recent contact with slope sediment regimes during its transport through the Irminger Sea. Therefore, the ^{230}Th concentration of NEADW is constrained both by recent boundary scavenging and equilibration with particles settling from the overlying LSW. ^{230}Th concentrations in DSOW also reflect a balance between recent con-

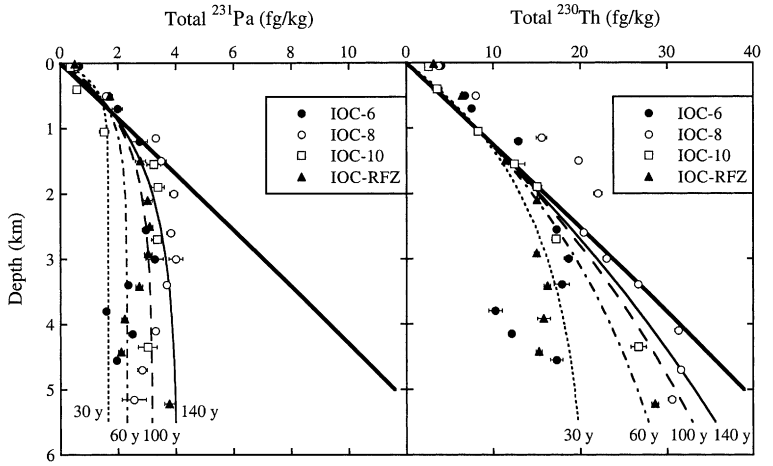

Fig. 7. Depth profiles of total ^{231}Pa and ^{230}Th concentration in the Equatorial and South Atlantic compared with the scavenging–mixing model (Eq. 2) for $\tau_w = 30$, 60, 100 and 140 years. Solid bold line is the linear increase in concentration with depth calculated assuming no advection.

tact with continental margin sediments and exchange with settling particles.

The vertical distribution of total ^{231}Pa in the Labrador Sea is also consistent with the calculated profile using the model parameters noted above, an average measured $K_{Pa} = 0.025$, and a water mass age of 12 yr (Fig. 6). The agreement between the water mass ages calculated using ^{231}Pa and ^{230}Th is encouraging, considering the different particle reactivity of these tracers. As noted above, these ages are consistent with CFC-12 ventilation ages for 'new' and 'old' LSW estimated by Azetsu-Scott et al. [34]. In addition, and unlike ^{230}Th, the low total ^{231}Pa concentration in the bottom water is consistent with the presence of younger Denmark Strait overflow water [34].

In the Equatorial and South Atlantic, calculated profiles using the scavenging model alone reproduce the observed increase in ^{231}Pa and ^{230}Th concentration down to ~1500–2000 m using the average measured K_{Pa} and K_{Th} values of 0.018 and 0.14, respectively (Fig. 7). Also, the agreement between the observations and model calculations in this depth range supports our use of $S = 500$ m/yr. Below these depths, the distributions of ^{231}Pa and ^{230}Th depart from the scavenging model prediction of a linear increase with depth. Application of the scavenging–mixing model (Eq. 2) is consistent with the majority of the ^{231}Pa and ^{230}Th data. The low ^{230}Th values at IOC-6 and IOC-8 between ~3500–4500 m most likely reflect the presence of multiple water masses that cannot be modeled as coming from a single source. Smethie et al. [36] have reported elevated CFC-11 concentrations between 3500 m and 4500 m on a section (J) close to IOC-6 associated with the presence of a mixture of NEADW and DSOW having a ventilation age of the order of 30–40 yr, values significantly lower compared to those of overlying waters.

The model results indicate a ~30–140 yr transit time from the northern source waters to this region of the western Atlantic (Fig. 7). Broecker et al. [37] reported radiocarbon measurements from ~40°N to 30°S that indicate rapid ventilation of the western Atlantic and comparatively slower penetration of ^{14}C into the interior of the basin. Their contoured ventilation ages for locations corresponding to our stations are between 80–160 yr, in good agreement with our results.

4.3. Meridional transport of ^{231}Pa and ^{230}Th in the Atlantic

Yu et al. [8] estimated that 51% of the ^{231}Pa and 11% of the ^{230}Th produced in the water column north of 25°N in the Atlantic was transported southwards by advection. This calculation was based on unpublished water column ^{231}Pa data and two low-resolution ^{230}Th profiles near the Nares and Hatteras Abyssal Plains [26]. A revised estimate of this transport can be made using our measured dissolved ^{231}Pa and ^{230}Th concentrations and the volume transports of 19.26 Sv northward above 1050 m and 19.17 Sv southward below 1050 m [8]. This calculation assumes no significant horizontal gradient in dissolved ^{231}Pa and ^{230}Th concentration between 25°N and the Equatorial and South Atlantic stations, which is reasonable considering the lack of any substantial horizontal gradients in the dissolved tracer profiles for the IOC-96 stations. This would further imply little change in water mass age within the latitudinal gradient from 25°N to 33°S.

Using our average measured dissolved ^{230}Th concentration of 6.5 fg/kg above 1050 m and 13.5 fg/kg below 1050 m, results in a transport of 1.33×10^{11} fg/s. This compares with a production rate of 1.37×10^{12} fg/s for the volume of seawater north of 25°N (7.7×10^{16} m^3), implying a net southward transport of 10% of the ^{230}Th produced and the remaining 90% removed by scavenging to the underlying sediments. For ^{231}Pa, using our average measured dissolved ^{231}Pa concentration of 1.1 fg/kg above 1050 m and 3.0 fg/kg below 1050 m results in a transport of 3.6×10^{10} fg/s, which corresponds to 68% of the ^{231}Pa produced north of 25°N (5.3×10^{10} dpm/s). Our results, based on direct measurement of these tracers in the water column, are consistent with Yu et al. [8] with respect to ^{230}Th, and suggest a ~17% upwards revision for the net southward meridional transport of ^{231}Pa in the Atlantic.

4.4. Implications for boundary scavenging in the Atlantic

The mass flux of particles and differential residence times of ^{231}Pa and ^{230}Th strongly influence the ^{231}Pa/^{230}Th deposition ratio in underlying sediments on a basin-wide scale. The extent of preferential lateral transport of less particle-reactive ^{231}Pa from low particle flux central gyres and eventual deposition in high particle flux areas (e.g., ocean margins and upwelling areas), referred to as boundary-scavenging [38,39], will also be a function of the age of intermediate/deep waters. In the relatively old deep waters of the Pacific, enhanced lateral transport of ^{231}Pa over ^{230}Th combined with scavenging removal from high particle flux regions results in excess sediment ^{231}Pa/^{230}Th ratios that may exceed the production ratio (0.093) [13,40]. This observation has led to the application of excess sediment ^{231}Pa/^{230}Th as a paleoproductivity index [41–46]. In the Atlantic, the residence time of intermediate/deep waters is similar to ^{231}Pa, and the net southward transport of this tracer has been suggested [7,8] to limit the preferential accumulation of ^{231}Pa in high particle flux regions and hence the magnitude of excess sediment ^{231}Pa/^{230}Th ratios in this basin.

The distributions of dissolved and particulate ^{231}Pa and ^{230}Th provide constraints on the extent of boundary scavenging in the Atlantic, which has implications for the use of excess sediment ^{231}Pa/^{230}Th as a tracer of past changes in the strength of Atlantic thermohaline circulation. Dissolved ^{231}Pa/^{230}Th ratios show no clear trend with latitude (Fig. 8a), with low and nearly uniform values evident in the Labrador Sea ($\sim$0.25), more scattered values in the Equatorial and South Atlantic (0.2–0.65), and decreasing values across the Antarctic Polar Front into the Southern Ocean ($\sim$0.3). These results indicate that dissolved ^{231}Pa/^{230}Th ratios are elevated prior to southward transport to the Southern Ocean [14,18,31,32].

In contrast to the dissolved data, particulate ^{231}Pa/^{230}Th ratios exhibit a strong latitudinal gradient (Fig. 8b), and more tightly constrained values within a station. Low particulate ^{231}Pa/^{230}Th ratios are observed in the Labrador Sea and the Equatorial and South Atlantic gyre extending

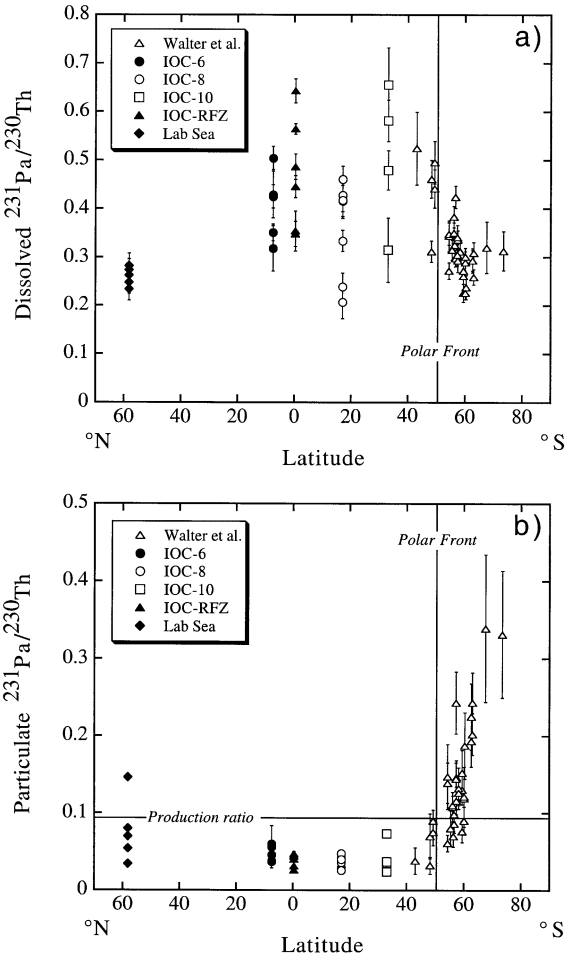

Fig. 8. Latitudinal dependence of (a) dissolved and (b) particulate ^{231}Pa/^{230}Th ratios in Atlantic intermediate and deep waters (1500 below surface, 500 m above ocean bottom). Triangles from Walter et al. [14].

down to 50°S, where they increase sharply across the Antarctic Polar Front (Fig. 8b). The average ^{231}Pa/^{230}Th activity ratio measured on all particulate samples from the Labrador Sea and IOC stations is 0.057 ± 0.003, well below the ^{231}Pa/^{230}Th production ratio (0.093) and in excellent agreement with low excess ^{231}Pa/^{230}Th ratios in Holocene sediments (0.060 ± 0.004) [8] and sediment trap material (0.034 ± 0.012) [31] from the Atlantic. The latitudinal variation in particulate ^{231}Pa/^{230}Th ratios is also consistent with ocean circulation-biogeochemistry model simulations of sedimentary ^{231}Pa/^{230}Th ratios [9], though our

water column data are insufficient to resolve the elevated sediment $^{231}Pa/^{230}Th$ ratios (~0.1) predicted for the Equatorial region (10°S–10°N).

Although no sediment $^{231}Pa/^{230}Th$ ratios have been reported for the Labrador Sea, our water column particulate data confirm that the low sedimentary $^{231}Pa/^{230}Th$ ratios observed between ~50°S–45°N [8,14] also hold for the Labrador Sea. It is important to obtain sedimentary $^{231}Pa/^{230}Th$ ratios where such data coverage is presently lacking; specifically, along the flow path of newly formed NADW, extending from the northern overflow waters, through the Labrador Sea and down to ~40°N. This northern North Atlantic regime, rather than the entire Atlantic basin [8], is where excess sediment $^{231}Pa/^{230}Th$ ratios are expected to be most responsive to changes in NADW production [7,9] and potentially resolve variations in the strength of NADW production through the last glacial termination.

An implication of the low water column particulate $^{231}Pa/^{230}Th$ ratios, which are well below the production ratio, is that boundary scavenging is indeed weakly expressed in the Atlantic [8,14,31]. Although it is possible that excess sediment $^{231}Pa/^{230}Th$ ratios may be similar to, or exceed, the production ratio in certain locations where boundary scavenging may be enhanced, such as the high productivity upwelling area off northern West Africa [8,9], these areas are very small and presently there is little evidence to suggest that this is the case. Also, our water column data are from regions more centrally located in the Atlantic, not from boundary areas. It is important to collect dissolved and particulate ^{231}Pa and ^{230}Th data from ocean margin regions to confirm that boundary scavenging is in fact suppressed throughout the entire Atlantic, as there may be undiscovered areas where there is a sink for ^{231}Pa other than the Southern Ocean. On a basin-wide scale, however, our water column data are consistent with the conclusion that the southward transport of newly formed NADW evidently limits the extent to which ^{231}Pa and ^{230}Th can be transported laterally by eddy diffusion from the low productivity central gyres to high particle flux marginal and upwelling regions.

In essence, the steady southward flow of NADW means that the Southern Ocean effectively becomes the 'boundary' at which Atlantic ^{230}Th and ^{231}Pa are removed. A key factor is that the residence time of Atlantic intermediate/deep waters (~100 yr [34]) and the timescale for lateral basin-wide mixing via eddy diffusion (~100 yr [8,47]) are similar to the scavenging residence time of ^{231}Pa (~50–200 yr). Based on our water column data, whereas only ~10% of the more particle-reactive ^{230}Th produced in the Atlantic is exported in southward flowing deep water [8], well over half (68%) of ^{231}Pa produced in situ is transported to the Southern Ocean. The southward transport of NADW is evidently of greater importance than scavenging in removing ^{231}Pa from the Atlantic water column down to ~50°S. There is therefore insufficient time for boundary scavenging to be fully expressed in the Atlantic, which is in marked contrast to the Pacific [40].

4.5. *Effect of particle composition on $^{231}Pa/^{230}Th$ ratios*

Particle composition can strongly influence particulate $^{231}Pa/^{230}Th$ ratios in the water column and underlying sediments and, hence, interpretations of boundary scavenging and past changes in deep water age [1,11,12,14,17–19]. An important question is the extent to which variations in particulate and excess sedimentary $^{231}Pa/^{230}Th$ ratios may reflect the differential adsorption of Pa and Th on particles of different geochemical composition as opposed to simply the total mass flux of particles. The extent to which particle composition may play a role in fractionating ^{231}Pa and ^{230}Th can be quantified using the fractionation factor $F_{Th/Pa}$:

$$F_{Th/Pa} = \frac{(^{230}Th/^{231}Pa)_{part}}{(^{230}Th/^{231}Pa)_{diss}} \quad (3)$$

Thus, our direct measurements of dissolved and particulate ^{231}Pa and ^{230}Th concentration can be used to gain further insight regarding the importance of particle geochemistry in controlling the latitudinal variation in $^{231}Pa/^{230}Th$ ratios in the water column as well as recorded in Atlantic sedi-

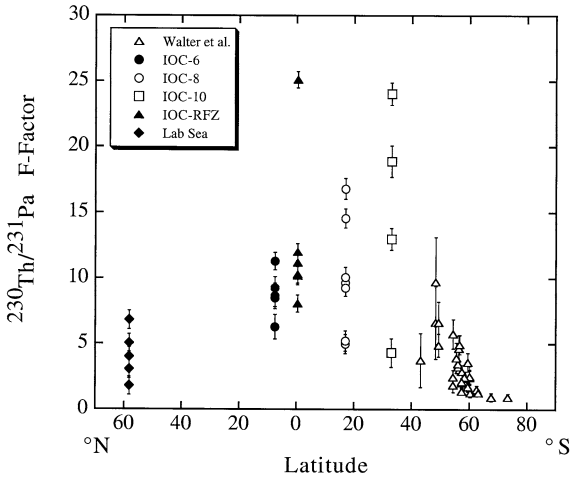

Fig. 9. Latitudinal dependence of ^{231}Pa/^{230}Th fractionation factor ($F_{Th/Pa}$) in Atlantic intermediate (1500 below surface) and deep waters (500 m above ocean bottom). Open triangles from Walter et al. [14].

ments [8,14]. As observed for particulate ^{231}Pa/^{230}Th ratios, there is a marked latitudinal dependence in particle fractionation of these tracers (Fig. 9). Elevated fractionation factors ($F_{Th/Pa}$) are observed near the Equator and South Atlantic gyre ($\sim$12), whereas much lower values are evident in the Labrador Sea ($\sim$3) and Southern Ocean ($\sim$2).

The latitudinal variations in $F_{Th/Pa}$ clearly indicate variable particle fractionation of ^{231}Pa and ^{230}Th, with more pronounced fractionation in the low-latitude regions (Fig. 9). These results can only be attributed to changes in the geochemical composition of the particulate matter controlling the removal of these tracers. Fractionation factors from laboratory experiments designed to investigate the adsorption of Th and Pa on different particle types in seawater indicate $F_{Th/Pa} \sim 1$–2 for Fe_2O_3, silica and MnO_2, and $\sim$9–12 for Al_2O_3 and natural lithogenic sediments [17]. By comparison, the observed particle fractionation of ^{231}Pa and ^{230}Th in the Equatorial and South Atlantic ($F_{Th/Pa} \sim 12$) is consistent with the predominantly lithogenic fluxes that characterize the majority of the Atlantic. The lack of fractionation between the particulate and dissolved phases south of the Antarctic Polar Front ($F_{Th/Pa} \sim 2$) has been suggested to be due to a greater proportion of silica (opal) in the Southern Ocean [14]. The Labrador Sea is also characterized by reduced fractionation ($F_{Th/Pa} \sim 3$), which indicates a change in particle geochemistry in this region, as opposed to a mass flux, since only the former can affect the fractionation factor. This striking observation may be a result of a higher proportion of diatoms, which generally increase with increasing primary productivity [48], and primary productivity was elevated in the upper 50 m during sampling in 1999 ($\sim$1–2.5 mmol C m^{-3} day^{-1}; G. Harrison, personal communication). Although we lack information on the silica content of these particles, inspection of the filters from the surface waters indicated the presence of diatom chains, suggesting that our sample collection coincided with a diatom bloom.

There also exists a marked depth dependence in $F_{Th/Pa}$, characterized by low values in the surface waters, a broad mid-depth maximum, and decreasing values towards the sea floor (Fig. 10). These results may reflect changes in the chemical composition of the particles which scavenge ^{231}Pa and ^{230}Th as they settle though the water column. This may be related to changes in particle geochemistry, or possible depth variations in particle remineralization. This suggestion is valid provided

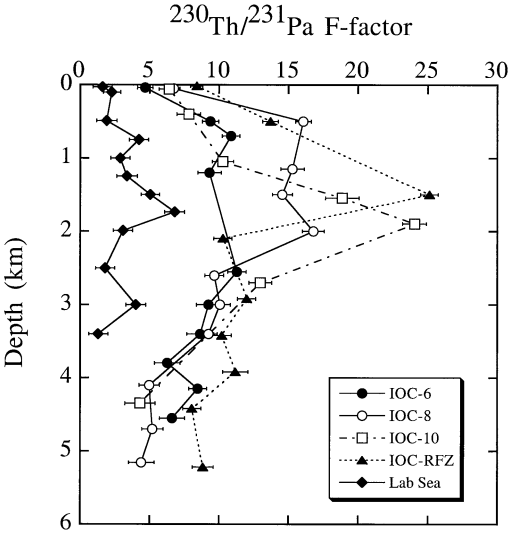

Fig. 10. Depth dependence of ^{231}Pa/^{230}Th fractionation factor ($F_{Th/Pa}$) in the Labrador Sea and Equatorial and South Atlantic.

that there exists an equilibrium exchange between dissolved and particulate forms with depth, as kinetic factors could decouple $F_{Th/Pa}$ from its local equilibrium value. Additional elemental analyses (e.g., Fe, Al, Mn, Si, Ca) should provide further insights regarding the relationship between particle geochemistry (lithogenic vs. biogenic) and variations in the $F_{Th/Pa}$ ratio of settling particles.

5. Conclusions

High precision water column measurements of dissolved and particulate ^{231}Pa and ^{230}Th in the Atlantic clearly indicate the importance of thermohaline circulation in controlling these tracers as they evolve in newly formed, southward flowing, intermediate/deep waters. Comparison of ^{231}Pa and ^{230}Th observations from 1993 and 1999 in the Labrador Sea confirms the changes in ventilation in this basin documented using CFC-11. The increase in total ^{230}Th in the Labrador Sea from 1993 to 1999 is consistent with aging of intermediate waters as a consequence of the cessation of deep convection in the Labrador Sea since 1993. Both ^{231}Pa and ^{230}Th tracer distributions indicate an intermediate/deep water age of 12 yr in the Labrador Sea and a 30–140 yr transit-time to low-latitude regions, consistent with CFC and bomb ^{14}C tracer distributions. The corresponding ^{231}Pa–^{230}Th water mass age estimates provide strong support for the use of these radionuclides as tracers of past changes in Atlantic thermohaline circulation.

The water column ^{231}Pa and ^{230}Th data provide a confirmation of the excess sediment $^{231}Pa/^{230}Th$ data in the Atlantic [8] and an improved estimate of the export of ^{231}Pa and ^{230}Th from the North Atlantic to the Southern Ocean. Average water column particulate $^{231}Pa/^{230}Th$ ratios are significantly below $^{231}Pa/^{230}Th$ production ratio and in excellent agreement with excess $^{231}Pa/^{230}Th$ ratios in Holocene (and LGM) sediments [8,14] and sediment trap material [31] in the Atlantic and model simulations [9]. On a basin-wide scale, water column particulate and sedimentary $^{231}Pa/^{230}Th$ ratios are consistent with the conclusion that the southward transport of newly formed NADW evidently limits the extent to which ^{231}Pa and ^{230}Th distributions are affected by lateral diffusion to the ocean margins. An implication is that the southward transport of deep water strongly attenuates boundary scavenging in the Atlantic and that $^{231}Pa/^{230}Th$ responds to changes in thermohaline circulation in this basin. In this regard, additional sedimentary $^{231}Pa/^{230}Th$ data should be obtained along the flow path of newly formed NADW, extending from the northern overflow waters through the Labrador Sea and down to $\sim$40°N. This northern Atlantic regime, rather than the entire Atlantic basin [8], is where excess sediment $^{231}Pa/^{230}Th$ ratios are expected to be most responsive to changes in NADW production [7,9] and potentially resolve variations in the strength of NADW production through the last glacial termination [8,9,15,16].

Particle fractionation of ^{231}Pa and ^{230}Th is clearly evident in the Atlantic and exhibits marked latitudinal and depth variations. The water column data from the Labrador Sea indicate that fractionation factors ($F_{Th/Pa}$) in this northern latitude basin can reach values as low as observed in the Southern Ocean, providing a new view of the extent of inter-basin variations in $^{231}Pa/^{230}Th$ fractionation. These results can only be attributed to changes in the geochemical composition of the particulate matter controlling the removal of these tracers. Down-core variations in $^{231}Pa/^{230}Th$ fractionation can potentially complicate the application of sedimentary $^{231}Pa/^{230}Th$ as a tracer of past changes in Atlantic thermohaline circulation. Further studies are required to better constrain the relationship between particle geochemistry (lithogenic vs. biogenic) and variations in the $F_{Th/Pa}$ ratio of settling particles.

Acknowledgements

We wish to acknowledge the support of the IOC, Chief Scientist G. Cutter, and M. Charette and B. Landing for sample collection. Allyn Clarke invited us to participate on the AR07W leg, and J. Dalziel and R. Nelson assisted with sample collection. Peter Jones allowed us access to his 1999 freon data. Michiel Rutgers van der

Loeff and an anonymous reviewer provided constructive comments. This work was funded by the NSF (OCE-9730257 to S.B.M. and H.N.E.; OCE-9731127 and EAR-9712037 to R.L.E.) and the Taiwan ROC NSC (NSC91-2116-M-006-004 to C.C.S.).*[BOYLE]*

References

[1] M.M. Rutgers van der Loeff, G.W. Berger, Scavenging of ^{230}Th and ^{231}Pa near the Antarctic Polar Front in the South Atlantic, Deep-Sea Res. I 40 (1993) 339–357.

[2] J.C. Scholten, M.M. Rutgers van der Loeff, A. Michel, Distribution of ^{230}Th and ^{231}Pa in the water column in relation to the ventilation of the deep Arctic basins, Deep-Sea Res. I 40 (1993) 339–357.

[3] H.N. Edmonds, S.B. Moran, J.A. Hoff, J.N. Smith, R.L. Edwards, Protactinium-231 and thorium-230 abundances and high scavenging rates in the western Arctic Ocean, Science 280 (1998) 405–407.

[4] S. Vogler, J. Scholten, M.M. Rutgers van der Loeff, A. Mangini, ^{230}Th in the Eastern North Atlantic: the importance of water mass ventilation in the balance of ^{230}Th, Earth Planet. Sci. Lett. 156 (1998) 61–74.

[5] S.B. Moran, J.A. Hoff, K.O. Buesseler, R.L. Edwards, High precision ^{230}Th and ^{232}Th in the Norwegian Sea and Denmark Strait by thermal ionization mass spectrometry, Geophys. Res. Lett. 22 (1995) 2589–2592.

[6] S.B. Moran, M.A. Charette, J.A. Hoff, R.L. Edwards, W.M. Landing, Distribution of ^{230}Th in the Labrador Sea in relation to ventilation, Earth Planet. Sci. Lett. 150 (1997) 151–160.

[7] S.B. Moran, C.-C. Shen, S.E. Weinstein, L.H. Hettinger, J.H. Hoff, H.N. Edmonds, R.L. Edwards, Constraints on deep water age and particle flux in the Equatorial and South Atlantic Ocean based on seawater ^{231}Pa and ^{230}Th data, Geophys. Res. Lett. 28 (2001) 3437–3440.

[8] E.-F. Yu, R. Francois, M.P. Bacon, Similar rates of modern and last-glacial ocean thermohaline circulation inferred from radiochemical data, Nature 379 (1996) 689–694.

[9] O. Marchal, R. Francois, T.F. Stocker, F. Joos, Ocean thermohaline circulation and sedimentary ^{231}Pa/^{230}Th ratio, Paleoceanography 15 (2000) 625–641.

[10] M.P. Bacon, R.F. Anderson, Distribution of thorium isotopes between dissolved and particulate forms in the deep sea, J. Geophys. Res. 87 (1982) 2045–2056.

[11] R.F. Anderson, M.P. Bacon, P.G. Brewer, Removal of ^{230}Th and ^{231}Pa at ocean margins, Earth Planet. Sci. Lett. 66 (1983) 73–90.

[12] R.F. Anderson, M.P. Bacon, P.G. Brewer, Removal of ^{230}Th and ^{231}Pa from the open ocean, Earth Planet. Sci. Lett. 62 (1983) 7–23.

[13] Y. Nozaki, T. Nakanishi, ^{231}Pa and ^{230}Th in the open ocean water column, Deep-Sea Res. I 32 (1985) 1209–1220.

[14] H.J. Walter, M.M. RutgersvanderLoeff, H. Hoeltzen, Enhanced scavenging of ^{231}Pa relative to ^{230}Th in the South Atlantic south of the Polar Front: implications for the use of the ^{231}Pa/^{230}Th ratio as a paleoproductivity proxy, Earth Planet. Sci. Lett. 149 (1997) 85–100.

[15] E.A. Boyle, Cadmium and δ^{13}C paleochemical ocean distributions during the stage 2 glacial maximum, Ann. Rev. Earth Planet. Sci. 20 (1992) 245–287.

[16] E.A. Boyle, Last-Glacial-Maximum North Atlantic Deep Water: on, off, or somewhere in between?, Philos. Trans. R. Soc. London Ser. B 348 (1995) 243–253.

[17] H.L. Andersen, R. Francois, S.B. Moran, Experimental evidence for differential adsorption of Th and Pa on different particle types in seawater, EOS Trans. Amer. Geophys. Union 73 (1992) 270.

[18] H.J. Walter, W. Geibert, M.M. Rutgers van der Loeff, G. Fischer, U. Bathmann, Shallow vs. deep-water scavenging of ^{231}Pa and ^{230}Th in radionuclide enriched waters of the Atlantic sector of the Southern Ocean, Earth Planet. Sci. Lett. 149 (2001) 85–100.

[19] S. Luo, T.-L. Ku, Oceanic ^{231}Pa/^{230}Th ratio influenced by particle composition and remineralization, Earth Planet. Sci. Lett. 167 (1999) 183–195.

[20] J.H. Chen, R.L. Edwards, G.J. Wasserburg, ^{238}U, ^{234}U and ^{232}Th in seawater, Earth Planet. Sci. Lett. 80 (1986) 241–251.

[21] R.L. Edwards, J.H. Chen, T.-L. Ku, G.J. Wasserburg, Precise timing of the last interglacial period from mass spectrometric determination of Th-230 in corals, Science 236 (1987) 1547–1553.

[22] R.L. Edwards, H. Cheng, M.T. Murrell, S.J. Goldstein, Protactinium-231 dating of carbonates by thermal ionization mass spectrometry: implications for Quaternary climate change, Science 276 (1997) 782–786.

[23] C.-C. Shen, R.L. Edwards, H. Cheng, J.A. Dorale, R.B. Thomas, S.B. Moran, S.E. Weinstein, H.N. Edmonds, Uranium and thorium isotopic and concentration measurements by magnetic sector inductively coupled plasma mass spectrometry, Chem. Geol. 185 (2002) 165–178.

[24] C.-C. Shen, R.L. Edwards, H. Cheng, R.B. Thomas, S.B. Moran, Attogram-sized ^{231}Pa analysis in seawater by isotope dilution mass spectroscopy, Anal. Chem. (in prep.) (2003).

[25] G.A. Cutter, C.I. Measures, The 1996 IOC contaminant baseline survey in the Atlantic Ocean from 33°S to 10°N: introduction, sampling protocols, and hydrographic data, Deep-Sea Res. II 46 (1999) 867–884.

[26] J.K. Cochran, H.D. Livingston, D.J. Hirschberg, L.D. Suprenant, Natural and anthropogenic radionuclide distributions in the northwest Atlantic Ocean, Earth Planet. Sci. Lett. 84 (1987) 135–152.

[27] G.M. Henderson, C. Heinze, R.F. Anderson, A.M.E. Winguth, Global distribution of the ^{230}Th flux to ocean sediments constrained by GCM modelling, Deep-Sea Res. I 46 (1999) 1861–1893.

[28] M.-S. Choi, R. Francois, K. Sims, M.P. Bacon, S. Brown-Leger, A.P. Fleer, L. Ball, D. Schneider, S. Pichat, Rapid determination of ^{230}Th and ^{231}Pa in seawater by desolvated-micronebulization inductively-coupled magnetic sector mass spectrometry, Mar. Chem. 76 (2001) 99–112.
[29] Y. Nozaki, H.-S. Yang, M. Yamada, Scavenging of thorium in the ocean, J. Geophys. Res. 92 (1987) C772–C778.
[30] M.P. Bacon, C.-A. Huh, A.P. Fleer, W.G. Deuser, Seasonality in the flux of natural radionuclides and plutonium in the deep Sargasso Sea, Deep-Sea Res. I 32 (1985) 273–286.
[31] E.-F. Yu, R. Francois, M.P. Bacon, A.P. Fleer, Fluxes of ^{230}Th and ^{231}Pa to the deep sea: implications for interpretation of excess ^{230}Th and ^{231}Pa/^{230}Th profiles in sediments, Earth Planet. Sci. Lett. 191 (2001) 865–889.
[32] E.-F. Yu, R. Francois, M.P. Bacon, S. Honjo, A.P. Fleer, S.J. Manganini, M.M. Rutgers van der Loeff, V. Ittekot, Trapping efficiency of bottom tethered sediment traps estimated from the intercepted fluxes of ^{230}Th and ^{231}Pa, Deep-Sea Res. I 48 (2001) 865–889.
[33] M.P. Bacon, C.-A. Huh, R.M. Moore, Vertical profiles of some natural radionuclides over the Alpha Ridge, Arctic Ocean, Earth Planet. Sci. Lett. 95 (1989) 15–22.
[34] K. Azetsu-Scott, E.P. Jones, R.M. Gershey, Transient tracers in the Labrador Sea, J. Geophys. Res. (in review) (2001).
[35] S.J. Walker, R.F. Weiss, P.K. Salameh, Reconstructed histories of the annual mean atmospheric mole fractions for the halocarbons CFC-11, CFC-12, CFC-113 and carbon tetrachloride, J. Geophys. Res. 105 (2000) 14285–14296.
[36] W.M. Smethie Jr., R.A. Fine, A. Putzka, E.P. Jones, Tracing the flow of North Atlantic Deep Water using chlorofluorocarbons, J. Geophys. Res. 105 (2000) 14297–14323.
[37] W.S. Broecker, S. Blanton, W.M. Smethie Jr., G. Ostlund, Radiocarbon decay and oxygen utilization in the deep Atlantic Ocean, Glob. Biogeochem. Cycl. 5 (1991) 87–117.
[38] M.P. Bacon, D.W. Spencer, P.G. Brewer, Pb-210/Ra-226 and Po-210/Pb-210 disequilibria in seawater and suspended matter, Earth Planet. Sci. Lett. 17 (1976) 295–305.
[39] M.P. Bacon, Tracers of chemical scavenging in the ocean: boundary effects and large-scale chemical fractionation, Phil. Trans. R. Soc. London Ser. A 325 (1988) 147–160.
[40] H.S. Yang, Y. Nozaki, H. Sakai, A. Masuda, The distribution of ^{230}Th and ^{231}Pa in the deep-sea surface sediments of the Pacific Ocean, Geochim. Cosmochim. Acta 50 (1986) 81–99.
[41] Y. Lao, R.F. Anderson, W.S. Broecker, Boundary scavenging and deep sea sediment dating: constraints from excess ^{230}Th and ^{231}Pa, Paleoceanography 7 (1992) 783–798.
[42] Y. Lao, R.F. Anderson, W.S. Broecker, S.E. Trumbore, H.J. Wolfli, Transport and burial rates of ^{10}Be and ^{231}Pa in the Pacific during the Holocene period, Earth Planet. Sci. Lett. 113 (1992) 173–189.
[43] N. Kumar, R. Gwiazda, R.F. Anderson, P.N. Froelich, ^{231}Pa/^{230}Th ratios in sediments as a proxy for past changes in Southern Ocean productivity, Nature 362 (1993) 45–48.
[44] N. Kumar, R.F. Anderson, R.A. Mortlock, P.N. Froelich, P. Kubik, B. Dittrich-Hannen, M. Suter, Increased biological productivity and export production in the glacial southern Ocean, Nature 378 (1995) 675–680.
[45] R. Francois, M.P. Bacon, M.A. Altabet, L.D. Labeyrie, Glacial/interglacial changes in sediment rain rate in the SW Indian sector of subantarctic waters as recorded by ^{230}Th, ^{231}Pa, U and δ^{15}N, Paleoceanography 8 (1993) 611–629.
[46] R. Francois, M.A. Altabet, E.-F. Yu, D.M. Sigman, M.P. Bacon, M. Frank, G. Bohrmann, G. Bareille, L.D. Labeyrie, Contribution of Southern Ocean upper water column stratification to the glacial decrease in atmospheric CO_2, Nature 389 (1997) 929–935.
[47] R.F. Anderson, Y. Lao, W.S. Broecker, S.E. Trumbore, H.J. Hoffman, W. Wolfli, Boundary scavenging in the Pacific Ocean: a comparison of ^{10}Be and ^{231}Pa, Earth Planet. Sci. Lett. 96 (1990) 287–304.
[48] D.M. Nelson, P. Treguer, M. Brezinski, A. Leynaert, B. Queguiner, Production and dissolution of biogenic silica in the ocean: revised global estimates, comparison with regional data and relationship to biogenic sedimentation, Glob. Biogeochem. Cycl. 9 (1995) 359–372.